THE INFLUENCE OF A LINEAR HYDROGEN CONCENTRATION GRADIENT ON FLAME ACCELERATION AND DEFLAGRATION-TO-DETONATION TRANSITION IN OBSTACLES

Shuo WANG[1,2*], Xinsheng JIANG[1], Qin HE[2], Yunxiong CAI[1], Yuxiang ZHOU[1], Tang TANG[1], Hongfu MI[3]

[1]Joint Logistics Support Force University of Engineering, Chongqing, 401311, China.

[2]School of Environmental Science and Safety Engineering, Tianjin University of Technology, Tianjin 300384, China.

[3]College of Safety Engineering, Chongqing University of Science and Technology, Chongqing 401331, China.

[*] Corresponding Author: wangs1102jz@163.com

This study investigates the influence of a linear hydrogen concentration gradient on flame acceleration and deflagration-to-detonation transition (DDT) within obstructed environments. This study employs numerical simulation methods to model the hydrogen flame propagation by coupling turbulence modeling with detailed chemical kinetics. The numerical framework accurately captures the coupled heat transfer behavior using the Euler time integration scheme with the HLLC flux scheme. A baseline hydrogen concentration of 30 vol% is established, featuring linear vertical concentration gradients characterized by slopes of 130.91, 205.72, and 480.00. The simulation results demonstrate that combustion reactions proceed more rapidly in high-concentration regions. This accelerated reaction rate, coupled with boundary layer instability effects, generates localized pressure and temperature gradients that subsequently enhance flame propagation velocity. The characteristic behavior manifests as an increased frequency of flame oscillation and acceleration with higher concentration gradient slopes. This relationship suggests a direct coupling between mixture stratification intensity and combustion instability. Furthermore, while the overdrive detonation velocity exhibits a positive correlation with the gradient slope, the stable detonation velocity remains relatively consistent, being primarily governed by the overall hydrogen concentration.

Keywords: *Premixed flame; DDT; Concentration gradient; Heat flow coupling; Numerical simulation*

1. Introduction

Hydrogen has emerged as a crucial strategic energy resource, simultaneously addressing two critical challenges: energy security and carbon neutrality. Furthermore, it serves as a catalyst for technological innovation and industrial transformation across multiple sectors [1, 2]. The widespread

adoption of hydrogen energy necessitates a comprehensive understanding of its safety considerations. Addressing these safety challenges is fundamental to realizing the full potential of hydrogen as a clean energy carrier [3]. Consequently, investigating hydrogen deflagration characteristics has become a critical research priority in the field of hydrogen safety.

Statistical analysis of historical hydrogen accidents reveals that deflagration events account for approximately 70% of reported incidents [4]. These findings underscore the critical importance of investigating hydrogen deflagration characteristics. Given the unique propensity of hydrogen for deflagration-to-detonation transition (DDT), numerical simulations have emerged as the primary investigative method, overcoming the inherent limitations of experimental approaches in studying its combustion behavior [5].

In confined environments, the ignition of hydrogen-air mixtures by high-temperature sources generates premixed flame front propagation. This combustion behavior exhibits distinct characteristics due to spatial constraints and mixture properties. Clanet *et al*. [6] first identified four distinct stages of flame propagation: spherical, finger-shaped, planar, and tulip flame formations. This seminal work established the foundation for subsequent investigations into premixed flame combustion dynamics. Building upon fundamental research, Middha *et al*. [7, 8] investigated the DDT process and established a predictive criterion. Their approach correlates geometric dimensions with detonation cell characteristics to assess DDT potential. Kim *et al*. [9] systematically investigated how flow dynamics and mixture concentration affect flame acceleration during DDT. Complementing this work, Sánchez *et al*. [10] comprehensively reviewed hydrogen flame characteristics, highlighting the critical roles of concentration gradients, ignition sources, and environmental conditions in deflagration behavior. Kuznetsov *et al*. [11] expanded the investigation by examining how obstacles and concentration gradients influence detonation overpressure. Their comprehensive analysis elucidated the external explosion mechanisms responsible for generating multi-peak pressure structures. Xiao *et al*. [12, 13] employed high-performance CFD simulations to investigate turbulent diffusion and heat transfer in hydrogen environments. Their study systematically analyzed flame acceleration phenomena, while elucidating the underlying mechanisms of premixed flame transformation into detonation waves. Furthermore, Wang *et al*. [14] examined the impact of obstacle configuration on DDT, demonstrating that symmetric obstacle arrangements yield minimal detonation distances and times. Complementing this research, Saeid *et al*. [15, 16] explored how hydrogen diffusion times affect DDT mechanisms in non-uniform mixtures.

In summary, existing literature on hydrogen detonation has systematically investigated flame dynamics phenomena. These include the findings that boundary constraints dominate flame acceleration and instability, as demonstrated by the author using fractal theory [17]. Moreover, the proposed continuous obstacles induce flow field disturbance, thereby forming a mutually reinforcing positive feedback mechanism[18, 19]. Previous studies have evidenced that the local Damköhler (Da) number undergoes drastic changes in the concentration gradient field, leading to the switching of flame propagation between the dynamic and the transport control region. This is the key factor driving flame instability and acceleration. Evidence indicates that positive concentration gradients along the flame propagation direction typically enhance DDT substantially, conversely, negative gradients tend to suppress or delay DDT [20]. However, earlier studies have neglected the influence of lateral hydrogen concentration gradients on flame acceleration in obstructed conditions.

This study quantitatively analyzes the overdriven detonation and stable detonation velocities

induced by hydrogen deflagration under varying concentration gradients, focusing on revealing the unique acceleration patterns of hydrogen flames triggered under obstructed conditions. By integrating flow characteristics with pressure field analysis, the flame acceleration mechanism is elucidated. These findings provide critical insights for developing effective thermal mitigation strategies across various hydrogen utilization scenarios.

2. Modeling and numerical methods

2.1. Governing equations and turbulence model

Flame propagation is fundamentally governed by the conservation laws of mass, momentum, and energy. These governing equations are expressed as follows [21, 22]:

$$\frac{\partial}{\partial t}\rho + \frac{\partial}{\partial x_i}(\rho u_i) = 0 \tag{1}$$

$$\frac{\partial}{\partial t}(\rho u_i) + \frac{\partial}{\partial x_j}\left(\rho u_i u_j\right) = -\frac{\partial p}{\partial x_i} + \frac{\partial \tau_{ij}}{\partial x_j} + \rho a \tag{2}$$

$$\frac{\partial}{\partial t}(\rho U_e) + \frac{\partial}{\partial x_j}\left[u_j(p + \rho U_e)\right] = \frac{\partial}{\partial x_j}\left(\tau_{ij} u_i\right) - \frac{\partial D_j}{\partial x_j} \tag{3}$$

$$\frac{\partial}{\partial t}(\rho N_m) + \frac{\partial}{\partial x_j}\left(\rho N_m u_j\right) = \frac{\partial}{\partial x_j}\left(\rho D_c \frac{\partial N_m}{\partial x_j}\right) + \omega_m \tag{4}$$

$$p = \rho R T \tag{5}$$

where t is time, s; ρ is density, kg/m^3; x_i is the position in the i direction, m; u_i is the velocity in the i direction, m/s; a is the external force acting on the fluid unit, N; p is pressure, Pa; U_e is the total internal energy，as $U_e = E + u_i u_i/2$, J; D_j is the diffusion term, ω_m is the net production rate of m in reaction, mol/L·s; D_c is the diffusion coefficient, m^2/s R is the gas constant, and T is the temperature K.

For detailed implementation steps, please refer to the preliminary study [18]. The turbulence characteristics are modeled using the SST k-ω, while flame propagation is described by the progress variable *c*:

$$\frac{\partial}{\partial t}(\bar{\rho}\tilde{c}) + \frac{\partial}{\partial x_j}\left(\bar{\rho}\tilde{c}\tilde{u}_j\right) = \frac{\partial}{\partial x_j}\left[\bar{\rho}\frac{\partial \tilde{c}}{\partial x_j}\left(D_c + \frac{\mu_{tap}}{\bar{\rho} Sc_T}\right)\right] + \bar{\omega}_{c,def} + \bar{\omega}_{c,ign} \tag{6}$$

where μ_{tap} is the apparent viscosity, Pa·s; Sc_T is the turbulent Schmidt number.

2.2. Detailed reaction mechanism

The hydrogen-air combustion chemistry is modeled using the detailed reaction mechanism developed by O'Conaire *et al*. [23], and the complete reaction scheme is presented in Tab. 1.

Table 1. H_2/O_2 Reaction Mechanism

Reaction numbers	Reactions	A	n	E
	H_2/O_2 chain reactions			
1	$\cdot H+O_2=\cdot O+\cdot OH$	1.91×10^{14}	0	16.44
2	$\cdot O+H_2=\cdot H+\cdot OH$	5.08×10^{4}	2.67	6.292
3	$\cdot OH+H_2=\cdot H+H_2O$	2.16×10^{8}	1.51	3.43
4	$\cdot O+H_2O=\cdot OH+\cdot OH$	2.97×10^{6}	2.02	13.4
	H_2/O_2 dissociation/recombination reactions			

5	$H_2+M=\cdot H+\cdot H+M$	4.57×10^{19}	-1.40	105.1
6	$\cdot O+\cdot O+M=O_2+M$	6.17×10^{15}	-0.50	0
7	$\cdot O+\cdot H+M=\cdot OH+M$	4.72×10^{18}	-1.00	0
8	$\cdot H+\cdot OH+M=H_2O+M$	4.50×10^{22}	-2.00	0
	Formation and consumption of $\cdot HO_2$			
9	$\cdot H+O_2+M=\cdot HO_2+M$	3.48×10^{16}	-0.41	-1.12
	$\cdot H+O_2=H\dot{O}_2$	1.48×10^{12}	0.60	0
10	$\cdot HO_2+\cdot H=H_2+O_2$	1.66×10^{13}	0	0.82
11	$HO_2+\dot{H}=\dot{O}H+\dot{O}H$	7.08×10^{13}	0	0.30
12	$\cdot HO_2+\cdot O=\cdot OH+O_2$	3.25×10^{13}	0	0
13	$\cdot HO_2+\cdot OH=H_2O+O_2$	2.89×10^{13}	0	-0.50
	Formation and consumption of H_2O_2			
14	$\cdot HO_2+HO_2=H_2O_2+O_2$	4.2×10^{14}	0	11.98
	$\cdot HO_2+\cdot HO_2=H_2O_2+O_2$	1.3×10^{11}	0	-1.629
15	$H_2O_2+M=\cdot OH+\cdot OH+M$	1.27×10^{17}	0	45.5
	$H_2O_2=\cdot OH+\cdot OH$	2.95×10^{14}	0	48.4
16	$H_2O_2+\cdot H=H_2O+\cdot OH$	2.41×10^{13}	0	3.97
17	$H_2O_2+\cdot H=H_2+\cdot HO_2$	6.03×10^{13}	0	7.95
18	$H_2O_2+\cdot O=\cdot OH+\cdot HO_2$	9.55×10^{6}	2.00	3.97
19	$H_2O_2+\cdot OH=H_2O+HO_2$	1.0×10^{12}	0	0
	$H_2O_2+\cdot OH=H_2O+\cdot HO_2$	5.8×10^{14}	0	9.56

2.3. Computational domain and geometry

The computational domain consists of a two-dimensional (2D) horizontal channel with dimensions of 3000 mm × 60 mm, which has been verified to induce a detonation transition [18]. A series of rectangular obstacles (15 mm×10 mm) is symmetrically set on the top and bottom walls, as illustrated in Fig. 1. The obstacles are spaced at 200 mm, resulting in a blockage ratio (BR) of 0.5. This length-to-diameter ratio (L/D) ensures the capture of DDT within the computational domain while corresponding to the elongated scenario of hydrogen transport. Structural blockages simulated in hydrogen transportation aim to elucidate the critical influence of turbulence and shock reflection on flame acceleration mechanisms. The uniformly structured meshes provide higher computational accuracy in capturing flame dynamics. This configuration allows for precise resolution of the flame front evolution and combustion characteristics [24].

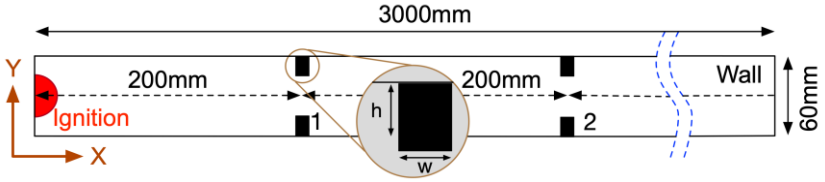

Figure 1. Schematic diagram of flame propagation domain

2.4. Boundary conditions

To accurately describe the physical explosion process, the following boundary conditions were

implemented: (1) The left boundary is defined as a non-slip, adiabatic solid wall. The ignition patch is initialized at this boundary to trigger the combustion process with 2400 K. (2) The top, bottom, and right boundaries, including the obstacle, are defined as non-slip, adiabatic walls. (3) The domain is initially filled with a baseline hydrogen concentration of 30 vol%. As shown in Fig. 2, the hydrogen concentration exhibits a linear distribution along the Y-axis, characterized by three distinct gradient slopes: L-1 = 130.91, L-2 = 205.72, and L-3 = 480.0. The initial pressure and temperature of the computational domain are 101325 Pa and 298 K.

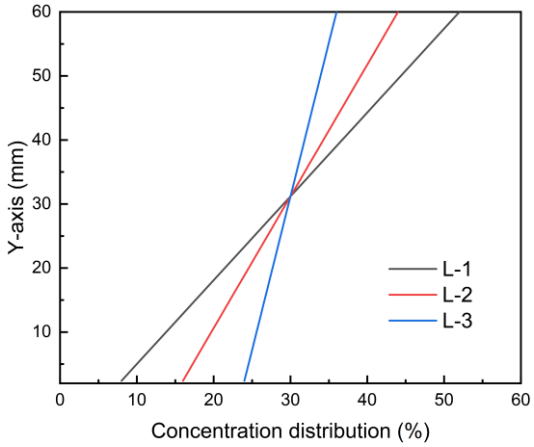

Figure 2. Distribution of hydrogen concentration

2.5. Numerical Schemes and Discretization

The governing equations are solved via the finite volume method (FVM). The computational domain is discretized using a structured mesh with a resolution of 0.5 mm. This resolution ensures that the flame and the induction zone behind the shock are captured with sufficient detail [24]. A first-order Euler scheme is utilized, where the time step dynamically controlled by a Courant-Friedrichs-Lewy (CFL) number of 0.2 to ensure numerical stability. The Harten-Lax-van Leer-Contact (HLLC) approximate Riemann solver is employed to compute the convective fluxes. This scheme is particularly robust for capturing the shocks inherent in detonation.

The modeling and computational analysis for this numerical simulation were completed on the OpenFOAM, with visualization processed through ParaView. The numerical simulations are performed using ddtFoam. The computational procedure for each time step is as follows: first, the density, viscosity, and chemical reaction rate are calculated based on the pressure, temperature, and reaction progress variable. Next, the transport equation for the reaction process variable is solved. The compressible N-S equations are solved using a density-based approach. Subsequently, the self-ignition delay time is updated based on the local temperature and pressure history. Finally, the time step is dynamically adjusted to maintain the maximum CFL number, ensuring stability for flame-chemistry interactions. Experimental validation of this methodology is provided in the previous research [18].

3. Flame acceleration and DDT mechanism

Fig. 3 presents the temporal evolution of the hydrogen flame under three distinct concentration gradients: (a) 130.91, (b) 205.72, and (c) 480.00. The analysis indicates that hydrogen concentration strongly influences flame thermal diffusion, resulting in distinct inclination of the flame front during propagation. This concentration-dependent behavior highlights the crucial role of mixture stratification

in flame dynamics. Moreover, the flame front inclination angle increases as the concentration gradient slope becomes shallower. This geometric configuration reduces thermal energy accumulation in the reaction zone, thereby slowing flame propagation. Meanwhile, thermal energy accumulation at the flame boundary promotes the formation of hot spot, establishing critical conditions for detonation within the heat-flow coupling region. This phenomenon results from turbulence-induced enhancement of concentration and temperature gradients within the boundary layer, which facilitates flame self-ignition. It is verified that strong temperature or concentration gradients lead to significant differences in local self-ignition delay times, thereby causing the gas compressed by shock waves to ignite at varying locations [25]. Steeper concentration gradients lead to faster flame propagation and shorter hot-spot formation durations. Specifically, the transition durations are 7.08 ms (out of 7.9 ms total), 6.32 ms (out of 7.21 ms total), and 5.06 ms (out of 6.09 ms total) for gradients L-1, L-2, and L-3.

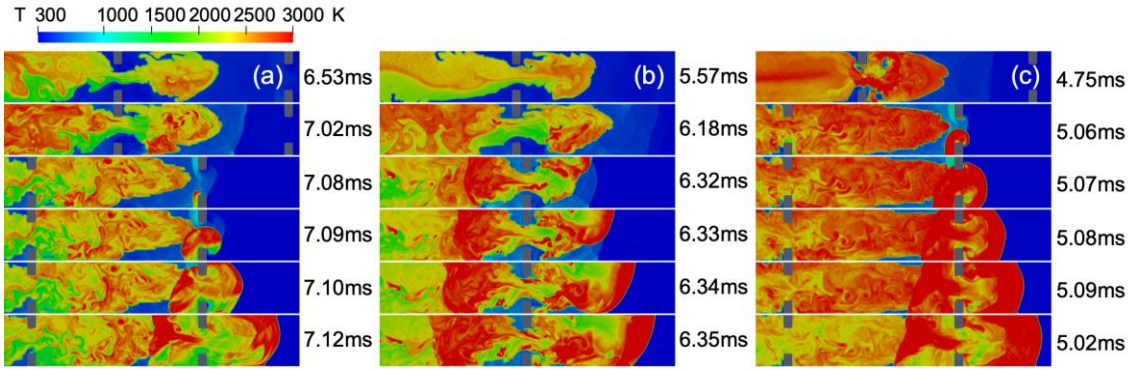

Figure 3. Results of dynamic flame propagation

Fig. 4 presents the temporal evolution of the flame front. The obstacle-induced stretching of the flame significantly increases the flame surface area between the flame boundary and the unburned gas, thereby enhancing combustion reactions and flame propagation. Obstacle-induced deformation of the shear layer triggers a transition from expansion-driven to flow-driven flame propagation. This transition is further amplified by the positive feedback between the flow field and the reaction zone, with flame acceleration between obstacles showing a clear dependence on concentration gradient. Specifically, steeper concentration gradients lead to faster flame front propagation. Exponential fitting results ($y_1=e^{2.75x}$, $y_2=e^{3.03x}$, $y_3=e^{3.75x}$) indicate a positive correlation between the concentration gradient and flame acceleration coefficient. This quantitative analysis demonstrates that steeper concentration gradients enhance acceleration effectiveness between obstacles.

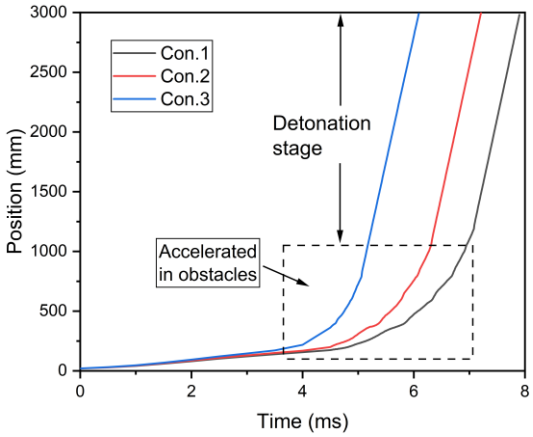

Figure 4. Position changes of the flame front

The evolution of flame velocity is calculated using the flame tip tracking method $v = (x + \Delta x)/(t + \Delta t)$, as shown in Fig. 5, allowing for precise tracking of flame dynamics. The flame acceleration process between obstacles exhibits an oscillatory upward trend. Notably, smoother concentration gradients amplify both the fluctuation frequency and amplitude of the flame velocity. This phenomenon is attributed to the intermittent coupling of thermal expansion and flow dynamics on flame acceleration. Under steeper concentration gradients, the synergistic interaction between turbulent transport and chemical heat release enhances flame propagation while reducing both the amplitude and frequency of flame-front velocity oscillations. This self-sustaining mechanism facilitates sustained flame acceleration throughout propagation. The interaction between flame and shock waves induces an overdriven detonation upon hot spot formation, facilitated by obstacle-induced turbulence and compression. This further confirms the mechanism by which obstacles accelerate the DDT process in non-uniform concentrations [25]. Specifically, the mixture composition behind the obstacle reaches stoichiometric conditions under high-velocity diffraction, thereby promoting DDT initiation. The analysis reveals a positive correlation between concentration gradient and detonation intensity, with measured overdriven detonation velocities of 1.40, 1.82, and 2.12 times the Chapman-Jouguet (CJ) velocity (D/D_{C-J}) for progressively steeper gradients. The stable detonation velocity is determined to be 1.06 times the C-J velocity (calculated using Cantera 3.0 [26] as 1979.1 m/s).

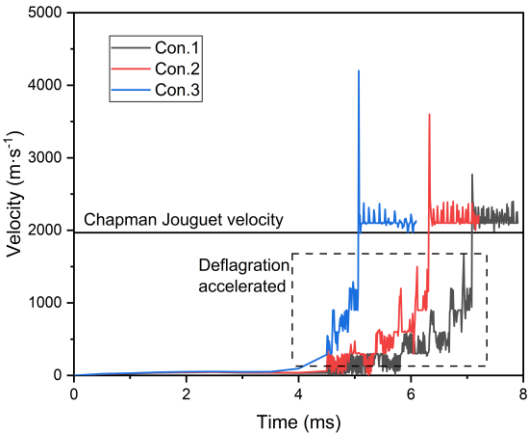

Figure 5. Flame propagation velocity

Fig. 6 illustrates the flame surface area during propagation, highlighting the strong dependence on concentration gradients. Smoother gradients induce significant combustion delays while promoting flame-front stretching through obstacle-induced shear layer shedding. The maximum observed flame-front areas are 0.56 m, 0.71 m, and 1.11 m for progressively smoothing gradients. This expansion disperses thermal energy, thereby reducing the efficiency of hot spot formation.

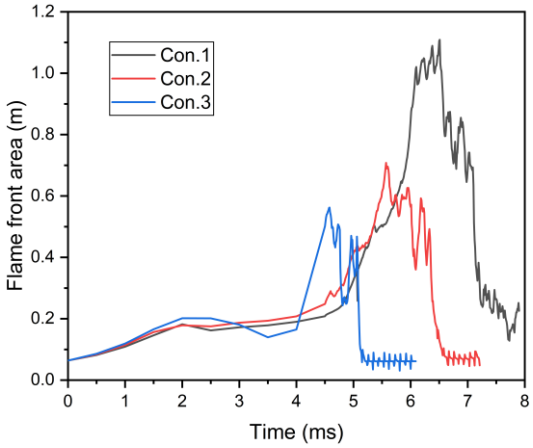

Figure 6. Flame front area

Fig. 7 presents the coupled evolution of combustion wave and precursor shock waves during DDT. The shear layers compress the flame front, enhancing both flame stretching and diffraction effects. Notably, smoother concentration gradients produce shock reflections predominantly from the bottom wall, while steeper gradients generate symmetric shock reflections from both walls. The Mach reflection formed on the side wall is classified primarily as a single Mach reflection (SMR), characterized by a Mach stem, a reflected shock waves, and a slip line, all intersecting at the triple point [25]. As transverse waves perpendicular to the wall surface, Mach stems generate regions with significantly higher local pressure and temperature than the incident shock. The hot spots originating from the triple point and behind the Mach stems act as highly reactive initiation kernels, substantially enhancing the chemical heat release rate and promoting the DDT process.

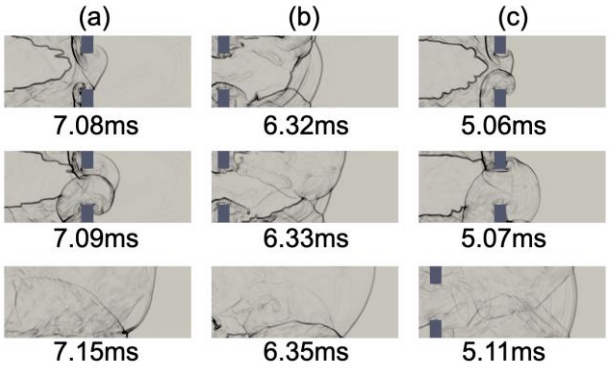

Figure 7. Evolution of detonation flame and shock wave

Fig. 8 demonstrates the critical influence of pressure-wave dynamics on flame acceleration and detonation. Shock-wave reflections off the obstacle generate localized high-pressure regions that that increase the local reaction rate. When coupled with flame diffraction around obstacles, these regions further intensify the chemical heat release. Notably, under high-gradient concentration conditions, localized pressure spikes form readily, with the resulting pressure gradients acting as the primary drivers for the hot spot. The positive feedback mechanism between pressure and flame velocity constitutes the primary driver of rapid pressure accumulation. This feedback mechanism is significantly intensified under conditions of steep concentration gradients, enhancing the coupling between pressure waves and chemical heat release rate. Consequently, this process accelerates DDT and facilitates stable detonation.

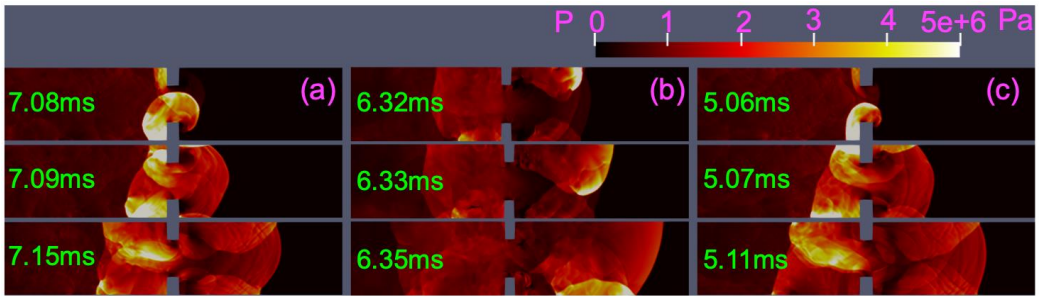

Figure 8. Pressure development during the DDT process

4. Deflagration and detonation: A comprehensive analysis for industrial safety

In industrial scenarios, hydrogen-air mixtures rarely remain in a quiescent and homogeneous state. Instead, these mixtures exhibit pronounced spatial concentration gradients. This study demonstrates that concentration gradients are the critical determinant of the transition from relatively controllable combustion/ignition to catastrophic detonation. Specifically, steeper concentration gradient slopes promote efficient DDT. From an industrial safety perspective, it is essential to focus not only on global hydrogen concentration but also on spatial distribution inhomogeneities. By promoting dilution to mitigate concentration gradients, the conditions conducive to efficient DDT can be disrupted.

Secondly, within pipelines or confined spaces, high-density arrangements of supports, valves, and other internal obstructions should be minimized in areas prone to hydrogen accumulation to prevent the rapid flame acceleration leading to DDT.

Conclusions

1. The acceleration of hydrogen premixed flame propagation during rapid flame acceleration is strongly dependent on concentration gradients. The coupling of flow instability with pressure accumulation mechanisms leads to distinct acceleration patterns and varied detonation initiation processes.

2. Smoother gradients induce increased induction delays, which creates temporal mismatches between heat release and accumulation that attenuate flame acceleration. Conversely, steeper gradients facilitate more efficient DDT.

3. Overdriven detonation velocities of 1.40, 1.82, and 2.12 times the C-J velocity were observed, corresponding to concentration gradient of 130.91, 205.72, and 480.00, respectively. Although concentration gradients and obstacle configurations affect flame acceleration, they exert a negligible influence on stable detonation phase. At a given average concentration, the hydrogen maintains a stable detonation velocity of 1.06 times the C-J velocity.

4. Premixed flames exhibit enhanced acceleration within localized pressure buildup regions. Under steep concentration gradient conditions, the positive feedback between the pressure and velocity fields is amplified, thereby accelerating the transition to detonation.

Acknowledgement

This work is supported by the National Natural Science Foundation of China (52274177). Scientific Research Foundation of Tianjin University of Technology (01002401). Thanks to DeepSeek

for providing language polishing support.

Conflict of interest

We have no conflicts of interest to disclose.

References

[1] Li, X., *et al*., Latest Approaches On Green Hydrogen As A Potential Source Of Renewable Energy Towards Sustainable Energy: Spotlighting Of Recent Innovations, Challenges, And Future Insights, *Fuel*, *334* (2023), pp. 126684

[2] Yang, J., *et al*., Liquid Hydrogen Refueling Stations: A Review On Process Layouts, Pump Technology, And Cold Energy Utilization, *Int. J. Hydrogen Energy*, *137* (2025), pp. 260-280

[3] Meziat Ramirez, F.A., *et al*., Numerical Study Of The Flame Acceleration Mechanisms Of A Lean Hydrogen/Air Deflagration In An Obstructed Channel, *Int. J. Hydrogen Energy*, *89* (2024), pp. 224-232

[4] The Joint Research Centre (JRC) of the European Commission, The Hydrogen Incident and Accidents Database, https://minerva.jrc.ec.europa.eu/en/shorturl/capri/hiadpt

[5] Saeid, M.H.S., *et al*., Numerical Investigation Of The Mechanism Behind The Deflagration To Detonation Transition In Homogeneous And Inhomogeneous Mixtures Of H2-Air In An Obstructed Channel, *Int. J. Hydrogen Energy*, *46* (2021), 41, pp. 21657-21671

[6] Clanet, C., Searby, G., On The “Tulip Flame” Phenomenon, *Combust. Flame*, *105* (1996), 1-2, pp. 225-238

[7] Middha, P., Hansen, O.R., Predicting Deflagration To Detonation Transition In Hydrogen Explosions, *Process Safety Progress*, *27* (2008), 3, pp. 192-204

[8] Rosas, C., *et al*., Deflagration To Detonation Transitions (DDTs): Predicting DDTs In Hydrocarbon Explosions, *J. Loss Prev. Process Ind.*, *30* (2014), 1, pp. 263-274

[9] Kim, W.K., *et al*., Flame Acceleration In Unconfined Hydrogen/Air Deflagrations Using Infrared Photography, *J. Loss Prev. Process Ind.*, *26* (2013), 6, pp. 1501-1505

[10] Sánchez, A.L., Williams, F.A., Recent Advances In Understanding Of Flammability Characteristics Of hydrogen, *Prog. Energy Combust. Sci.*, *41* (2014), 1, pp. 1-55

[11] Kuznetsov, M., *et al*., Medium-Scale Experiments On Vented Hydrogen Deflagration, *J. Loss Prev. Process Ind.*, *36* (2015), pp. 416-428

[12] Xiao, H., Fan, J., DDT Run-Up Distance In Uniform And Non-Uniform Hydrogen–Air Mixtures In Sparsely-Obstructed Channels, *Combust. Flame*, *273* (2025), pp. 113919

[13] Liu, Z., *et al*., Flame Acceleration And DDT In A Channel With Fence-Type Obstacles: Effect Of Obstacle Shape And Arrangement, *Proceedings of the Combustion Institute*, *39* (2023), 3, pp. 2787-2796

[14] Wang, J., *et al*., Effect Of Solid Obstacle Distribution On Flame Acceleration And DDT In

Obstructed Channels Filled with Hydrogen-Air Mixture, *Int. J. Hydrogen Energy*, *47* (2022), 25, pp. 12759-12770

[15] Saeid, M.H.S., *et al*., Effect Of Diffusion Time On The Mechanism Of Deflagration To Detonation Transition In An Inhomogeneous Mixture Of Hydrogen-Air, *Int. J. Hydrogen Energy*, *47* (2022), 55, pp. 23411-23426

[16] Saeid, M.H.S., *et al*., Numerical Study On The Effects Of Obstacle Shape And Thickness On Deflagration-To-Detonation Transition In Hydrogen–Air Mixtures With A Transverse Concentration Gradient, *Case Studies in Thermal Engineering*, *66* (2025), pp. 105726

[17] Wang, S., *et al*., Effect Of Obstacle Arrangement On Premixed Hydrogen Flame: Eddy-Dissipation Concept Model Based Numerical Simulation, *Int. J. Hydrogen Energy*, *48* (2023), 43, pp. 16445-16456

[18] Wang, S., *et al*., Effect Of Blockage Mode On Hydrogen Deflagration To Detonation Transition In A Long And Narrow Space, *Thermal Science*, (2025), 00, pp. 218-218

[19] Wang, S., *et al*., Numerical Simulation Of The Behavior And Mechanism Of Premixed Hydrogen Flame Acceleration In Continuous Disturbance, *Combustion Science and Technology*, (2026)

[20] Fan, J., *et al*., Effect Of Concentration Gradient On DDT And Detonation Front Dynamics In A Closed Combustion Channel, *Appl. Therm. Eng.*, *278* (2025)

[21] Ettner, F., *et al*., Numerical Simulation Of The Deflagration-To-Detonation Transition In Inhomogeneous Mixtures, *Journal of Combustion*, *2014* (2014), 1, pp. 686347

[22] Wang, J., *et al*., Effects Of The Quantity And Arrangement Of Reactive Jet Obstacles On Flame Acceleration And Transition To Detonation: A Numerical Study, *Aerosp. Sci. Technol.*, *137* (2023), pp. 108269

[23] O'Conaire, M., *et al*., A Comprehensive Modeling Study Of Hydrogen Oxidation, *Int. J. Chem. Kinet.*, *36* (2004), pp. 603-622

[24] Vohra, U., *et al*., Numerical Study Of Deflagration To Detonation Transition In 2D And Axisymmetric Detonation Tube With Obstacles Using OpenFOAM, *Lecture Notes in Mechanical Engineering*, (2021), pp. 807-820

[25] Yang, Z., Zhang, B., Typical Onset Modes Of DDT And Behavior Of Strong Transverse Shocks, *Chinese Journal of Aeronautics*, *39* (2026), 3

[26] Goodwin, D.G., *et al*., Cantera: An Object-Oriented Software Toolkit For Chemical Kinetics, Thermodynamics, And Transport Processes

Submitted: 30.01.2026.
Revised: 14.03.2026.
Accepted: 16.03.2026.